Computers & Fluids 46 (2011) 312–317

Contents lists available at ScienceDirect

Computers & Fluids

journal homepage: www.elsevier.com/locate/compfluid

Synchronized flux corrected remapping for ALE methods

Richard Liska [a,*], Mikhail Shashkov [b], Pavel Váchal [a], Burton Wendroff [b]

[a] Czech Technical University in Prague, Faculty of Nuclear Sciences and Physical Engineering, Břehová 7, 115 19 Prague 1, Czech Republic
[b] Los Alamos National Laboratory, Applied Mathematics & Plasma Physics Group (T-5), Los Alamos, NM 87545, USA

ARTICLE INFO

Article history:
Received 30 April 2010
Received in revised form 9 November 2010
Accepted 16 November 2010
Available online 21 November 2010

Keywords:
ALE
FCT
Remapping

ABSTRACT

A new optimization-based synchronized flux corrected conservative interpolation (remapping) of mass, momentum and energy for arbitrary Lagrangian Eulerian method is developed. Fluxes of conserved variables (mass, momentum and total energy) are limited in a synchronous FCT-like way to preserve local bounds in density, velocity and specific internal energy.

1. Introduction

The arbitrary Lagrangian Eulerian (ALE) method [1] is widely used in hydrodynamical fluid flow modeling. It consists of several Lagrangian steps followed by rezoning and remapping steps. Rezoning step smooths the Lagrangian mesh to prevent its distortion and remapping performs conservative interpolation of the conserved quantities from the old Lagrangian mesh to the new rezoned one. To minimize interpolation errors one needs to use the high-order remapping, which however tends to produce overshoots or undershoots (i.e. creates new local extrema) in the vicinity of discontinuities. Creation of the new local extrema can be reduced by using slope limiters during reconstruction phase of the remapping [2], however this approach in general cannot avoid new local extrema. To remove the new local extrema one typically employs some a posterior procedure such as repair [3] which distributes the excessive conservative quantity into the neighboring cells.

To avoid this a-posteriori correction we propose a new remapping method, based on the flux corrected transport (FCT) ideas [4–6], which does not produce new local extrema. The new flux corrected remap (FCR) is local by definition (one interface at a time), simple and fast. Its extension to general multidimensional meshes is easy. The FCT type methods have been applied to system of Euler equations by either FCT limiting of characteristic variables [7,8] or by using the same limiter (being the minimum of density and energy or density and pressure limiters) for all equations [9,10], which is sometimes called synchronized. By synchronized we however understand something else. We have three independent FCR limiters for conserved mass, momentum and energy and we choose these limiters in such a way that the remapped solution satisfies bounds in density, velocity and internal energy and our FCR solution stays close to the high-order solution. Schär and Smolarkiewicz [11] apply the synchronized FCT method to the system of transport equations and we compare our FCR with remapping based on their method. In the FCR method we guarantee the bounds in density, velocity and specific internal energy (internal energy per unit mass) by constraining the fluxes of mass, momentum and total energy. We employ independent flux limiting correction factors for mass, momentum and total energy. From the bounds we derive the constraints on the correction factors. The constrained optimization chooses the correction factors satisfying the constraints which are in some sense optimal, i.e. producing fluxes close to the high-order fluxes. Compared to the sequential FCR [12], we apply the bounds simultaneously to treat all quantities in the system at once, thus we call our method synchronized FCR (SFCR). The SFCR method has been developed in [13] for mass and momentum with bounds in density and velocity. Here we extend it to include also remap of total energy with bounds in internal energy.

2. Problem statement

The underlying functions describing the fluid at position $\mathbf{r}$ are density $\rho(\mathbf{r})$, velocity $\mathbf{u}(\mathbf{r})$, specific internal energy $\varepsilon(\mathbf{r})$ and total energy $e(\mathbf{r}) = \rho(\varepsilon + \mathbf{u}^2/2)$. The rezoning phase of the ALE method constructs from the old Lagrangian mesh Ω (consisting of cells Ω_i) the new rezoned mesh $\tilde{\Omega}$ (consisting of cells $\tilde{\Omega}_i$). The volume V_i, mass m_i, momentum $\boldsymbol{\mu}_i$ and total energy E_i of the old mesh cells

* Corresponding author.
E-mail address: liska@siduri.fjfi.cvut.cz (R. Liska).

0045-7930/$ - see front matter © 2010 Elsevier Ltd. All rights reserved.
doi:10.1016/j.compfluid.2010.11.013

Ω_i are given by $V_i = \int_{\Omega_i} dV$, $m_i = \int_{\Omega_i} \rho\, dV$, $\boldsymbol{\mu}_i = \int_{\Omega_i} \rho \mathbf{u}\, dV$, $E_i = \int_{\Omega_i} e\, dV$, and define the mean values of density, velocity and internal energy in the old mesh cells Ω_i as $\rho_i = m_i/V_i$, $\mathbf{u}_i = \boldsymbol{\mu}_i/m_i$, $\varepsilon_i = E_i/m_i - \mathbf{u}_i^2/2$.

Now given the mean values of density, velocity and internal energy on the old mesh, our task is to remap mass m, momentum $\boldsymbol{\mu}$ and total energy E to the new cell $\widetilde{\Omega}_i$, i.e. to compute approximations of

$$\tilde{m}_i \approx \tilde{m}_i^{\mathrm{e}} = \int_{\widetilde{\Omega}_i} \rho\, dV, \quad \tilde{\boldsymbol{\mu}}_i \approx \tilde{\boldsymbol{\mu}}_i^{\mathrm{e}} = \int_{\widetilde{\Omega}_i} \rho \mathbf{u}\, dV,$$
$$\widetilde{E}_i \approx \widetilde{E}_i^{\mathrm{e}} = \int_{\widetilde{\Omega}_i} \rho\left(\varepsilon + \frac{\mathbf{u}^2}{2}\right) dV,$$

which would give us the mean values of density, velocity and internal energy on the new mesh $\tilde{\rho}_i = \tilde{m}_i/\widetilde{V}_i, \tilde{\mathbf{u}}_i = \tilde{\boldsymbol{\mu}}_i/\tilde{m}_i, \tilde{\varepsilon}_i = \widetilde{E}_i/\tilde{m}_i - \tilde{\mathbf{u}}_i^2/2$. The basic requirements for the remapping are conservation, bounds preservation (weaker notion of monotonicity preservation) and accuracy. The remapping has to conserve mass, momentum and total energy, i.e.

$$\sum_i \tilde{m}_i = \sum_j m_j, \quad \sum_i \tilde{\boldsymbol{\mu}}_i = \sum_j \boldsymbol{\mu}_j, \quad \sum_i \widetilde{E}_i = \sum_j E_j.$$

To avoid creation/amplification of local extrema we require the remapped values to preserve local bounds in density, velocity and internal energy, i.e.

$$\rho_i^{\min} \leqslant \tilde{\rho}_i \leqslant \rho_i^{\max}, \quad \mathbf{u}_i^{\min} \leqslant \tilde{\mathbf{u}}_i \leqslant \mathbf{u}_i^{\max}, \quad \varepsilon_i^{\min} \leqslant \tilde{\varepsilon}_i \leqslant \varepsilon_i^{\max},$$

where

$$\rho_i^{\min} = \min_{\mathscr{N}(\Omega_i)} \rho_j, \quad \mathbf{u}_i^{\min} = \min_{\mathscr{N}(\Omega_i)} \mathbf{u}_j, \quad \varepsilon_i^{\min} = \min_{\mathscr{N}(\Omega_i)} \varepsilon_j,$$
$$\rho_i^{\max} = \max_{\mathscr{N}(\Omega_i)} \rho_j, \quad \mathbf{u}_i^{\max} = \max_{\mathscr{N}(\Omega_i)} \mathbf{u}_j, \quad \varepsilon_i^{\max} = \max(\max_{\mathscr{N}(\Omega_i)} \varepsilon_j, \tilde{\varepsilon}_i^L).$$

The max/min's are taken over the set $\mathscr{N}(\Omega_i)$ of cells neighboring the cell Ω_i, which includes the cell Ω_i. Typically this set $\mathscr{N}(\Omega_i)$ is defined as a set of cells which share with the cell Ω_i at least one node. The new low-order internal energy $\tilde{\varepsilon}_i^L = \widetilde{E}_i^L/\tilde{m}_i^L - 1/2\left(\tilde{\boldsymbol{\mu}}_i^L/\tilde{m}_i^L\right)^2$ (where $\tilde{m}_i^L$, $\tilde{\boldsymbol{\mu}}_i^L$, $\widetilde{E}_i^L$ are defined by (1) and its analogs for $\tilde{\boldsymbol{\mu}}_i^L$, $\widetilde{E}_i^L$) has to be included to guarantee that the low-order approximation stays in bounds (remapping of the velocity can decrease the kinetic energy which might lead to the increase of internal energy). For accuracy we require to remain high-order in smooth regions, which means that a linear function should be remapped exactly.

We assume that the rezone stage does not change the connectivity of the mesh and that it produces only small node displacement. Then the problem can be formulated in the flux form

$$\tilde{m}_i = m_i + \sum_{k\in\mathscr{M}(\Omega_i)} F_{i,k}^m, \quad \tilde{\boldsymbol{\mu}}_i = \boldsymbol{\mu}_i + \sum_{k\in\mathscr{M}(\Omega_i)} \mathbf{F}_{i,k}^{\mu}, \quad \widetilde{E}_i = E_i + \sum_{k\in\mathscr{M}(\Omega_i)} F_{i,k}^E$$

where $F_{k,i}^m = -F_{i,k}^m$, $\mathbf{F}_{k,i}^{\mu} = -\mathbf{F}_{i,k}^{\mu}$, $F_{k,i}^E = -F_{i,k}^E$ and the summation now goes over the set $\mathscr{M}(\Omega_i)$ of cells neighboring the cell Ω_i excluding the cell Ω_i. One can choose $\mathscr{M}(\Omega_i) = \mathscr{N}(\Omega_i) - \Omega_i$ or choose $\mathscr{M}(\Omega_i)$ as a set of cells Ω_k, $k \neq i$ which share one side (node in 1D, edge in 2D, face in 3D) with the cell Ω_i. The latter is our choice here. Our task is to find the suitable fluxes $F_{k,i}^m$, $\mathbf{F}_{k,i}^{\mu}$, $F_{k,i}^E$ on each interface (i,k) between cells i and k.

3. Principle of flux corrected remap for mass/density

The basic idea of flux corrected remap follows closely flux corrected transport [4–6]. We have a low-order (donor) and a high-order remap scheme

$$\tilde{m}_i^L = m_i + \sum_{k\in\mathscr{M}(\Omega_i)} F_{i,k}^{m,L}, \qquad \tilde{m}_i^H = m_i + \sum_{k\in\mathscr{M}(\Omega_i)} F_{i,k}^{m,H}, \tag{1}$$

where the low-order one preserves bounds. The flux corrected remap (FCR) scheme is then given by (for brevity from here further on we abbreviate the summation over $k \in \mathscr{M}(\Omega_i)$ by summation over k)

$$\tilde{m}_i^{\mathrm{FCR}} = m_i + \sum_k F_{i,k}^{m,\mathrm{FCR}}, \qquad F_{i,k}^{m,\mathrm{FCR}} = F_{i,k}^L + C_{i,k}^m\left(F_{i,k}^{m,H} - F_{i,k}^{m,L}\right)$$

and the question is how to choose correction factors $0 \leqslant C_{i,k}^m \leqslant 1$ for which the remapped values satisfy the bounds. Such correction factor always exists as the low-order scheme (obtained for $C_{i,k}^m = 0$) preserves the local bounds.

With anti-diffusive fluxes $dF_{i,k}^m = F_{i,k}^{m,H} - F_{i,k}^{m,L}$ the new mass obtained by FCR can be written as

$$\tilde{m}_i^{\mathrm{FCR}} = m_i + \sum_k F_{i,k}^{m,\mathrm{FCR}} = \tilde{m}_i^L + \sum_k C_{i,k}^m dF_{i,k}^m.$$

The density constraints $\rho_i^{\min} \leqslant \tilde{\rho}_i \leqslant \rho_i^{\max}$ are transformed into mass constraints $m_i^{\min} \leqslant \tilde{m}_i \leqslant m_i^{\max}$ which can be rewritten using the anti-diffusive fluxes as

$$m_i^{\min} - \tilde{m}_i^L \leqslant \sum_k C_{i,k}^m dF_{i,k}^m \leqslant m_i^{\max} - \tilde{m}_i^L. \tag{2}$$

The sum in these constraints is split into two parts according to the sign of the anti-diffusive fluxes, so that the right-hand (max) inequality is written as

$$\sum_k C_{i,k}^m dF_{i,k}^m = \sum_{dF_{i,k}^m>0} C_{i,k}^m dF_{i,k}^m + \sum_{dF_{i,k}^m<0} C_{i,k}^m dF_{i,k}^m \leqslant m_i^{\max} - \tilde{m}_i^L = Q_i^{m,\max} \geqslant 0.$$

The worst-case scenario is in the case when $\forall k,\ dF_{i,k}^m \geqslant 0$, in other words the sufficient condition for the upper (max) constraint is

$$\sum_{dF_{i,k}^m>0} C_{i,k}^m dF_{i,k}^m \leqslant Q_i^{m,\max}.$$

Similarly, the sufficient condition for the lower (min) constraint is

$$0 \geqslant m_i^{\min} - \tilde{m}_i^L = Q_i^{m,\min} \leqslant \sum_{dF_{i,k}^m<0} C_{i,k}^m dF_{i,k}^m.$$

In each cell, we define the incoming and outgoing total anti-diffusive fluxes $P^{m,+} = \sum_{dF_{i,k}^m>0} dF_{i,k}^m \geqslant 0$, $P^{m,-} = \sum_{dF_{i,k}^m<0} dF_{i,k}^m \leqslant 0$ and for nonzero $P^{m,+}$, resp. $P^{m,-}$ the auxiliary values $D_i^{m,+} = Q_i^{m,\max}/P_i^{m,+} \geqslant 0$, $D_i^{m,-} = Q_i^{m,\min}/P_i^{m,-} \geqslant 0$. Now if $C_{i,k}^m \leqslant D_i^{m,+}$ for $dF_{i,k}^m > 0$ and $C_{i,k}^m \leqslant D_i^{m,-}$ for $dF_{i,k}^m < 0$ then the mass bounds (2) are satisfied. At the interface (i,k) we have to apply the sufficient conditions for bounds in both neighboring cells i and k. So if for $dF_{i,k}^m > 0$ we choose $C_{i,k}^{m,\rho} = \min(D_i^{m,+}, D_k^{m,-}, 1)$ and for $dF_{i,k}^m < 0$ we choose $C_{i,k}^{m,\rho} = \min(D_i^{m,-}, D_k^{m,+}, 1)$ then the density bounds (2) are satisfied for any $0 \leqslant C_{i,k}^m \leqslant C_{i,k}^{m,\rho}$. Note that if $P_i^{m,+} = 0$ or $P_i^{m,-} = 0$, then corresponding D_i^m are not used and can remain undefined.

4. Synchronized FCR for density and momentum

Just as for the mass, we define the momentum anti-diffusive fluxes by $\mathbf{dF}_{i,k}^{\mu} = \mathbf{F}_{i,k}^{\mu,H} - \mathbf{F}_{i,k}^{\mu,L}$. The FCR momentum flux is now given by $\mathbf{F}_{i,k}^{\mu,\mathrm{FCR}} = \mathbf{F}_{i,k}^{\mu,L} + C_{i,k}^{\mu}\mathbf{dF}_{i,k}^{\mu}$ and the new FCR momentum is, as for the mass,

$$\tilde{\boldsymbol{\mu}}_i^{\mathrm{FCR}} = \boldsymbol{\mu}_i + \sum_k \mathbf{F}_{i,k}^{\mu,\mathrm{FCR}} = \tilde{\boldsymbol{\mu}}_i^L + \sum_k C_{i,k}^{\mu}\mathbf{dF}_{i,k}^{\mu}.$$

Note that even when velocity, momentum and its fluxes are vectors we use the scalar limiting factor $C_{i,k}^{\mu}$ as we do not want to

affect the vectors' directions by limiting. The local bounds on velocity are $\mathbf{u}_i^{\min} \leqslant \tilde{\mathbf{u}}_i \leqslant \mathbf{u}_i^{\max}$, where the vector inequalities are taken component by component. Velocity is a derived quantity and the velocity bounds $\mathbf{u}_i^{\min} \leqslant \tilde{\boldsymbol{\mu}}_i/\tilde{m}_i \leqslant \mathbf{u}_i^{\max}$ are rewritten as constraints on new momentum and mass $\tilde{m}_i\mathbf{u}_i^{\min} \leqslant \tilde{\boldsymbol{\mu}}_i \leqslant \tilde{m}_i\mathbf{u}_i^{\max}$ which, after insertion of fluxes, reads

$$\left(\tilde{m}_i^L + \sum_k C_{i,k}^m dF_{i,k}^m\right)\mathbf{u}_i^{\min} \leqslant \left(\tilde{\boldsymbol{\mu}}_i^L + \sum_k C_{i,k}^\mu \mathbf{dF}_{i,k}^\mu\right) \leqslant \left(\tilde{m}_i^L + \sum_k C_{i,k}^m dF_{i,k}^m\right)\mathbf{u}_i^{\max}.$$

This is a coupled system of linear inequalities with respect to unknown correction factors $C_{i,k}^m$, $C_{i,k}^\mu$ at all interfaces (i,k). We want to stay as close as possible to high-order fluxes, i.e. choose $C_{i,k}^m$, $C_{i,k}^\mu$ as close to one as possible. This is a global optimization problem, to maximize $C_{i,k}^m$, $C_{i,k}^\mu$ satisfying given linear constraints. The FCR strategy is used to approximate the global optimization problem by a sequence of local problems. The synchronized FCR (SFCR) method, outlined below, keeps inequalities coupled.

The right-hand (max) inequality can be written as

$$\sum_k \left(C_{i,k}^\mu \mathbf{dF}_{i,k}^\mu - \mathbf{u}_i^{\max} C_{i,k}^m dF_{i,k}^m\right) \leqslant \mathbf{u}_i^{\max}\tilde{m}_i^L - \tilde{\boldsymbol{\mu}}_i^L = \mathbf{Q}_i^{\mu,\max} \geqslant 0. \tag{3}$$

We denote the corrected contribution from the face (i,k) to the left-hand side of (3) by

$$\boldsymbol{\Phi}_{i,k}^{i,\mu,\max} = C_{i,k}^\mu \mathbf{dF}_{i,k}^\mu - \mathbf{u}_i^{\max} C_{i,k}^m dF_{i,k}^m$$

and the corresponding uncorrected quantity by

$$\boldsymbol{\Psi}_{i,k}^{i,\mu,\max} = \mathbf{dF}_{i,k}^\mu - \mathbf{u}_i^{\max} dF_{i,k}^m,$$

so that inequality (3) now reads

$$\sum_k \boldsymbol{\Phi}_{i,k}^{i,\mu,\max} \leqslant \mathbf{Q}_i^{\mu,\max}.$$

Similarly as for density, we subdivide the sum into two parts according to the sign of $\boldsymbol{\Psi}_{i,k}^{i,\mu,\max}$

$$\sum_{k;\boldsymbol{\Psi}_{i,k}^{i,\mu,\max}\leqslant 0} \boldsymbol{\Phi}_{i,k}^{i,\mu,\max} + \sum_{k;\boldsymbol{\Psi}_{i,k}^{i,\mu,\max}>0} \boldsymbol{\Phi}_{i,k}^{i,\mu,\max} \leqslant \mathbf{Q}_i^{\mu,\max}$$

and the sufficient conditions for this inequality are

$$\sum_{k;\boldsymbol{\Psi}_{i,k}^{i,\mu,\max}\leqslant 0} \boldsymbol{\Phi}_{i,k}^{i,\mu,\max} \leqslant 0, \qquad \sum_{k;\boldsymbol{\Psi}_{i,k}^{i,\mu,\max}>0} \boldsymbol{\Phi}_{i,k}^{i,\mu,\max} \leqslant \mathbf{Q}_i^{\mu,\max}. \tag{4}$$

The sufficient condition for the first resp. second inequality from (4) are

$$\boldsymbol{\Phi}_{i,k}^{i,\mu,\max} \leqslant 0 \quad \text{for} \quad \boldsymbol{\Psi}_{i,k}^{i,\mu,\max} \leqslant 0, \tag{5}$$

$$\boldsymbol{\Phi}_{i,k}^{i,\mu,\max} \leqslant \mathbf{D}_{i,k}^{\mu,\max,+}\boldsymbol{\Psi}_{i,k}^{i,\mu,\max} \quad \text{for} \quad \boldsymbol{\Psi}_{i,k}^{i,\mu,\max} > 0,$$

where $\mathbf{D}_{i,k}^{\mu,\max,+} = \mathbf{Q}_i^{\mu,\max}/\mathbf{P}_i^{\mu,\max,+}$ and $\mathbf{P}_i^{\mu,\max,+} = \sum_{\Psi>0}\boldsymbol{\Psi}_{i,k}^{i,\mu,\max}$ (all inequalities, arithmetic operations and sums of vectors are taken component by component). The derived constraints are linear in the correction factors $C_{i,k}^m$, $C_{i,k}^\mu$ and local, i.e. they are constraints on the interface (i,k) which are sufficient for the maximum velocity bound in the cell i. Similar derivation for the minimum velocity bound gives another set of constraints. The complete set of constraints for interface (i,k) includes constraints derived from both max/min velocity bounds in both cells i and k sharing the interface (i,k), the constraints $0 \leqslant C_{i,k}^m \leqslant C_{i,k}^{m,\rho}$ derived in the previous section from density bounds and the constraints $0 \leqslant C_{i,k}^\mu \leqslant 1$. The solution of the complete system of linear inequalities for $C_{i,k}^m$ and $C_{i,k}^\mu$ is a non-empty ($(C_{i,k}^m, C_{i,k}^\mu) = (0,0)$ corresponding to the low-order remap always satisfies all the constraints) convex polygon in $(C_{i,k}^m, C_{i,k}^\mu)$ space. Now the task is to find a pair $(C_{i,k}^m, C_{i,k}^\mu)$ that is in some sense optimal, producing a remap close to the high-order one, i.e. with $(C_{i,k}^m, C_{i,k}^\mu)$ close to (1,1). We minimize the functional

$$f\left(C_{i,k}^m, C_{i,k}^\mu\right) = -C_{i,k}^m \left\|dF_{i,k}^m\right\| \left(\frac{1}{\rho_i} + \frac{1}{\rho_k}\right) - C_{i,k}^\mu \left\|\mathbf{dF}_{i,k}^\mu\right\| \left(\frac{1}{\|\rho_i\mathbf{u}_i\| + \epsilon} + \frac{1}{\|\rho_k\mathbf{u}_k\| + \epsilon}\right), \tag{6}$$

where ϵ is a small quantity, under the derived constraints on $(C_{i,k}^m, C_{i,k}^\mu)$. The functional is proportional to the local L_1 deviation of the SFCR remapped density and momentum from the high-order ones. This minimization is local, i.e. done for each interface (i,k) separately. The minimum is always in one of the polygon's vertices, the polygon is intersection of eight half-planes (given by linear constraints), so the minimization in this case is easy. For more details on synchronized FCR for density and momentum see [13], where the choice of dimensional factors in a global deviation (the global analog of (6)) is made to produce a local minimization problem which is computationally efficient. Sensitivity to the choice of dimensional factors has not been investigated.

5. Synchronized FCR for density, momentum and energy

Just as for the mass and momentum we first define the total energy anti-diffusive fluxes by $\mathbf{dF}_{i,k}^E = \mathbf{F}_{i,k}^{E,H} - \mathbf{F}_{i,k}^{E,L}$. The FCR energy flux is now given by $\mathbf{F}_{i,k}^{E,\mathrm{FCR}} = \mathbf{F}_{i,k}^{E,L} + C_{i,k}^\mu \mathbf{dF}_{i,k}^E$ and the new FCR total energy is

$$\widetilde{E}_i^{\mathrm{FCR}} = E_i + \sum_k F_{i,k}^{E,\mathrm{FCR}} = \widetilde{E}_i^L + \sum_k C_{i,k}^E dF_{i,k}^E.$$

The local bounds on specific internal energy are $\varepsilon_i^{\min} \leqslant \tilde{\varepsilon}_i \leqslant \varepsilon_i^{\max}$ or $\varepsilon_i^{\min} \leqslant \widetilde{E}_i/\tilde{m}_i - \tilde{\mathbf{u}}_i^2/2 \leqslant \varepsilon_i^{\max}$. We rewrite the bounds in conserved quantities and get

$$\tilde{m}_i^2\varepsilon_i^{\min} \leqslant \widetilde{E}_i\tilde{m}_i - \frac{\tilde{\boldsymbol{\mu}}_i^2}{2} \leqslant \tilde{m}_i^2\varepsilon_i^{\max}.$$

The maximum internal energy bound, after insertion of fluxes, reads

$$\left(\widetilde{E}_i^L + \sum_k C_{i,k}^E dF_{i,k}^E\right)\left(\tilde{m}_i^L + \sum_k C_{i,k}^m dF_{i,k}^m\right) - \frac{1}{2}\left(\tilde{\boldsymbol{\mu}}_i^L + \sum_k C_{i,k}^\mu \mathbf{dF}_{i,k}^\mu\right)^2 \leqslant \varepsilon_i^{\max}\left(\tilde{m}_i^L + \sum_k C_{i,k}^m dF_{i,k}^m\right)^2. \tag{7}$$

We rearrange this inequality to get all $C's$ to the left-hand side

$$\sum_k \left\{ C_{ik}^E \left[dF_{ik}^E(\tilde{m}_i^L + C_{ik}^m dF_{ik}^m) + \sum_{l\neq k} C_{il}^m dF_{ik}^E dF_{il}^m\right] - C_{ik}^\mu \left[\mathbf{dF}_{ik}^\mu \cdot \left(\tilde{\boldsymbol{\mu}}_i^L + \frac{1}{2}C_{ik}^\mu \mathbf{dF}_{ik}^\mu\right) + \frac{1}{2}\sum_{l\neq k} C_{il}^\mu \mathbf{dF}_{ik}^\mu \cdot \mathbf{dF}_{il}^\mu\right] + C_{ik}^m \left[dF_{ik}^m(\widetilde{E}_i^L - \varepsilon_i^{\max}(2\tilde{m}_i^L + C_{ik}^m dF_{ik}^m))) - \varepsilon_i^{\max}\sum_{l\neq k} C_{il}^m dF_{ik}^m dF_{il}^m\right]\right\} \leqslant \varepsilon_i^{\max}(\tilde{m}_i^L)^2 - \widetilde{E}_i^L\tilde{m}_i^L + \frac{1}{2}(\tilde{\boldsymbol{\mu}}_i^L)^2 = Q_i^{E,\max} \geqslant 0 \tag{8}$$

To get a suitable sufficient condition for (8) we increase its left hand side (the part before $\leqslant$) by neglecting the negative (or positive as appropriate according to the sign) parts of the sums over l and setting $C_{il}^* = 1$ in these sums. So the sufficient condition for (8) is

$$\sum_k \left\{ C^E_{ik}\left[dF^E_{ik}(\tilde{m}^L_i + C^m_{ik} dF^m_{ik}) + \sum_{l\neq k}^{+} dF^E_{ik} dF^E_{il} \right] - C^\mu_{ik}\left[dF^\mu_{ik}\left(\tilde{\mu}^L_i + \frac{1}{2} C^\mu_{ik} dF^\mu_{ik} \right) + \frac{1}{2} \sum_{l\neq k}^{-} dF^\mu_{ik} dF^\mu_{il} \right] + C^m_{ik}\left[dF^m_{ik}(\tilde{E}^L_i - \varepsilon^{\max}_i (2\tilde{m}^L_i + C^m_{ik} dF^m_{ik}))) - \varepsilon^{\max}_i \sum_{l\neq k}^{-} dF^m_{ik} dF^m_{il} \right] \right\} \leqslant Q^{E,\max}_i \tag{9}$$

where

$$\sum_l^{+} x_{ikl} = \sum_{x_{ikl}>0} x_{ikl}, \quad \sum_l^{-} x_{ikl} = \sum_{x_{ikl}<0} x_{ikl}.$$

We define corrected $\Phi^{i,E,\max}_{ik}$ and uncorrected $\Psi^{i,E,\max}_{ik}$ contribution from face (i,k) to the left-hand side of (9) by

$$\begin{aligned}\Phi^{i,E,\max}_{ik}(C^m_{ik}, C^\mu_{ik}, C^E_{ik}) = {} & C^E_{ik}\left[dF^E_{ik}(\tilde{m}^L_i + C^m_{ik} dF^m_{ik}) + \sum_{l\neq k}^{+} dF^E_{ik} dF^m_{il} \right] \\ & - C^\mu_{ik}\left[dF^\mu_{ik}(\tilde{\mu}^L_i + \frac{1}{2} C^\mu_{ik} dF^\mu_{ik}) + \frac{1}{2} \sum_{l\neq k}^{-} dF^\mu_{ik} dF^\mu_{il} \right] \\ & + C^m_{ik}\left[dF^m_{ik}\left(\tilde{E}^L_i - \varepsilon^{\max}_i (2\tilde{m}^L_i + C^m_{ik} dF^m_{ik}) \right) \right) \\ & - \varepsilon^{\max}_i \sum_{l\neq k}^{-} dF^m_{ik} dF^m_{il} \Big],\end{aligned}$$

$$\Psi^{i,E,\max}_{ik} = \Phi^{i,E,\max}_{ik}(1,1,1).$$

Similarly as for velocity constraints we split the sum in the energy constraint (9) into two parts according to the sign of $\Psi^{i,E,\max}_{ik}$

$$\sum_{k;\Psi^{i,E,\max}_{ik}\leqslant 0} \Phi^{i,E,\max}_{ik} + \sum_{k;\Psi^{i,E,\max}_{ik}>0} \Phi^{i,E,\max}_{ik} \leqslant Q^{E,\max}_i$$

and the sufficient conditions for this inequality are

$$\sum_{k;\Psi^{i,E,\max}_{i,k}\leqslant 0} \Phi^{i,E,\max}_{i,k} \leqslant 0, \quad \sum_{k;\Psi^{i,E,\max}_{i,k}>0} \Phi^{i,E,\max}_{i,k} \leqslant Q^{E,\max}_i. \tag{10}$$

The sufficient conditions for the first resp. second inequality from (10) are

$$\begin{aligned}&\Phi^{i,E,\max}_{i,k} \leqslant 0 \quad \text{for } \Psi^{i,E,\max}_{i,k} \leqslant 0, \\ &\Phi^{i,E,\max}_{ik} \leqslant D^{E,\max,+}_{ik} \Psi^{i,E,\max}_{ik} \quad \text{for } \Psi^{i,E,\max}_{ik} > 0,\end{aligned} \tag{11}$$

where $D^{E,\max,+}_{ik} = Q^{E,\max}_i / P^{E,\max,+}_i$ and $P^{E,\max,+}_i = \sum_{\Psi>0} \Psi^{i,E,\max}_{i,k}$ (note that $D^{E,\max,+}_{ik}$ is needed only when $\Psi^{i,E,\max}_{ik} > 0$ which implies that $P^{E,\max,+}_i > 0$ and $D^{E,\max,+}_{ik}$ is well defined). The sufficient conditions (11) for the maximum energy constraint (7) in the cell i are non-linear constraints in the correction factors $(C^m_{ik}, C^\mu_{ik}, C^E_{ik})$ on the interface (i,k). In a similar way one derives the sufficient conditions for the minimum energy constraint.

Let us summarize the constraints on the unknown correction factors $(C^m_{ik}, C^\mu_{ik}, C^E_{ik})$ on the interface (i,k). First, to stay between the low-order and high-order fluxes we require $0 \leqslant C^m_{ik} \leqslant 1$, $0 \leqslant C^\mu_{ik} \leqslant 1$, $0 \leqslant C^E_{ik} \leqslant 1$. Next, from the density bounds we derived in Section 3, the constraint $C^m_{ik} \leqslant C^{\rho,m}_{ik} \leqslant 1$. Further, we derived two (min/max) linear constraints (5) in (C^m_{ik}, C^μ_{ik}) from the velocity bounds in cell i and we have to apply similar two (min/max) constraints from velocity bounds in cell k. Finally we have to include two (min/max) nonlinear constraints of type (11) in $(C^m_{ik}, C^\mu_{ik}, C^E_{ik})$ from energy bounds in cell i and also two more such constraints from energy bounds in cell k. Remembering that we want to stay close to the high-order scheme (i.e. maximize C's) we first try if $(C^m_{ik}, C^\mu_{ik}, C^E_{ik}) = (C^{\rho,m}_{ik}, 1, 1)$ satisfies all constraints and if it does we use on the interface (i,k) these values (which is probably the case in smooth regions where we avoid optimization). Otherwise we minimize the local deviation from the high-order fluxes given by the functional

$$\begin{aligned}f(C^m_{ik}, C^\mu_{ik}, C^E_{ik}) = {} & -C^m_{ik} \left\| dF^m_{ik} \right\| \left(\frac{1}{\rho_i} + \frac{1}{\rho_k} \right) \\ & - C^\mu_{ik} \left\| \mathbf{dF}^\mu_{ik} \right\| \left(\frac{1}{\|\mathbf{n}_i\| + \epsilon} + \frac{1}{\|\mathbf{n}_k\| + \epsilon} \right) \\ & - C^E_{ik} \left\| dF^E_{ik} \right\| \left(\frac{1}{e_i} + \frac{1}{e_k} \right),\end{aligned}$$

where $\mathbf{n}_i = \rho_i \mathbf{u}_i$ and $e_i = \rho_i(\varepsilon_i + \mathbf{u}_i^2/2)$, under all derived constraints on $(C^m_{ik}, C^\mu_{ik}, C^E_{ik})$. So on each interface (i,k) we get one constrained minimization problem which gives us the SFCR correction factors.

6. Numerical tests

In this section we present several numerical tests showing the performance of the developed synchronized FCR for density, momentum and energy. For the tests we use the 1D cyclic remapping [2] defined by the sequence of meshes generated using the analytical function

$$\begin{aligned}&x(\xi,t) = x_{\min} + (x_{\max} - x_{\min})\tilde{\xi}(\xi,t), \\ &\tilde{\xi}(\xi,t) = [1-\alpha(t)]\xi + \alpha(t)\xi^2, \\ &\alpha(t) = \frac{\sin(4\pi t)}{2}, \quad 0 \leqslant \xi \leqslant 1,\ 0 \leqslant t \leqslant 1.\end{aligned} \tag{12}$$

The mesh node positions $\{x^k_i\}$ are defined as $x^k_i = x(\xi_i, t^k) = x((i-1)/N, k/k_{\max})$ with $k = 0,\ldots,k_{\max}$ corresponding to pseudo-time steps and $i = 1,\ldots,N+1$ corresponding to spatial node positions. Here N is the number of spatial cells and $k_{\max}$ is the total number of pseudo-time steps. The rate of convergence is tested by refining the resolution $(N, k_{\max}) = (64,320)$, $(128,640)$,

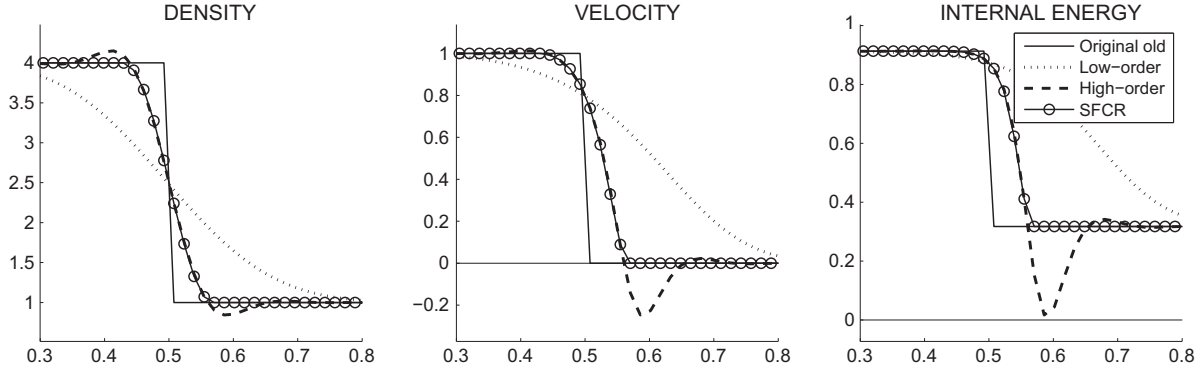

Fig. 1. Simple shock with 64 cells after 320 remaps by high-order, low-order and SFCR schemes.

(256,1280). The given variables (ρ,u,ε) are initially defined on the initial uniform mesh. In each pseudo-time step the mesh at t^k is moved to the new position given by the new pseudo-time t^{k+1} and the variables are remapped to the new mesh. The last mesh at pseudo-time $t^{k_{\max}}$ is the same as the first initial uniform mesh, so the exact solution is given by the initial profile and we can compute errors of approximate remap and its convergence rate.

6.1. Simple shock

The first test is a simple shock connecting two constant states. Initial (and exact final) density, velocity and internal energy profiles are given by

$$(\rho,u,\varepsilon)(x) = \begin{cases} (4,1,115/126) & \text{for} \quad 0 \leqslant x \leqslant 0.5, \\ (1,0,20/63) & \text{for} \quad 0.5 < x \leqslant 1. \end{cases}$$

The final result after 320 cyclic remaps on the mesh (12) with 64 cells is shown in Fig. 1 computed by the low-order , high-order and SFCR schemes. Clearly the low-order scheme is too diffusive, the high-order scheme produces overshoots and undershoots while SFCR scheme does produce neither overshoots nor undershoots while keeping the same gradient at the shock as the high-order scheme. The table of convergence is presented in Table 1 which also includes results by Schär and Smolarkiewicz (S&S) method [11] for density and velocity (S&S paper does not deal with internal energy bounds). For the description of S&S remapping and

Table 1
Convergence tables (L_1 errors and their ratios) in density, velocity and internal energy for cyclic remapping of simple shock by low-order, high-order, SFCR and S&S methods.

Method	Resolution		L_1 error			Err. prev./curr. resol.		
	N	$k_{\max}$	ρ	u	ε	ρ	u	ε
Low-order	64	320	0.121	0.262	0.158			
	128	640	0.086	0.186	0.112	1.4	1.4	1.4
	256	1280	0.061	0.131	0.080	1.4	1.4	1.4
High-order	64	320	0.038	0.093	0.064			
	128	640	0.022	0.055	0.038	1.7	1.7	1.7
	256	1280	0.013	0.033	0.023	1.7	1.7	1.7
SFCR	64	320	0.030	0.062	0.036			
	128	640	0.018	0.037	0.022	1.7	1.7	1.7
	256	1280	0.011	0.022	0.013	1.7	1.7	1.7
S&S	64	320	0.035	0.078	–			
	128	640	0.023	0.049	–	1.5	1.6	–
	256	1280	0.015	0.032	–	1.5	1.5	–

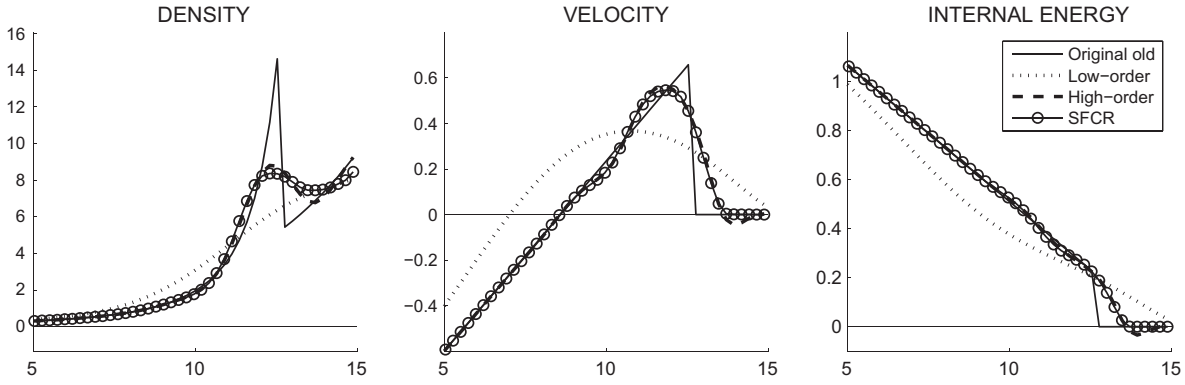

Fig. 2. Exponential shock with 64 cells after 320 remaps by high-order, low-order and SFCR schemes.

Table 2
Convergence tables (L_1 errors and their ratios) in density, velocity and internal energy for cyclic remapping of exponential shock by low-order, high-order, SFCR and S&S methods.

Method	Resolution		L_1 error			Err. prev./curr. resol.		
	N	$k_{\max}$	ρ	u	ε	ρ	u	ε
Low-order	64	320	0.257	0.341	0.119			
	128	640	0.190	0.205	0.068	1.4	1.7	1.7
	256	1280	0.163	0.128	0.040	1.2	1.6	1.7
High-order	64	320	0.122	0.056	0.014			
	128	640	0.068	0.030	0.008	1.8	1.9	1.7
	256	1280	0.046	0.018	0.005	1.5	1.7	1.6
SFCR	64	320	0.151	0.049	0.012			
	128	640	0.078	0.025	0.006	1.9	2.0	2.0
	256	1280	0.047	0.014	0.004	1.7	1.7	1.6
S&S	64	320	0.213	0.083	–			
	128	640	0.134	0.039	–	1.6	2.1	–
	256	1280	0.095	0.022	–	1.4	1.8	–

its comparison with SFCR see [13]. The SFCR method produces smaller errors than both high-order and S&S methods. The SFCR order of convergence is the same as that for the high-order method.

6.2. Exponential shock

The second test is an exponential shock with initial (and exact final) density, velocity and internal energy profiles given by

$$(\rho,u,\varepsilon)(x)=\begin{cases}\left(3\rho_0\exp\left(\frac{x_F-x_0}{\delta}\right)(1+2\eta)^{-\frac{5}{2}},\frac{1-\eta}{t}\delta,\frac{\delta^2}{t^2}(1+2\eta)\right) & \text{for } 0\leqslant x\leqslant x_F,\\ \left(\rho_0\exp\left(\frac{x-x_0}{\delta}\right),0,0\right) & \text{for } x_F<x\leqslant 15.\end{cases}$$

where $x_F=x_0+\frac{3}{2}\delta\log(t/t_0)$, $\eta=\frac{x_F-x}{\delta}$, $t_0=2$, $x_0=6$, $\rho_0=1$, $\delta=4$, $t=6$. The final result after 320 cyclic remaps on the mesh (12) with 64 cells is shown in Fig. 2 computed by the low-order, high-order and SFCR schemes. The low-order scheme smears the peak in density completely, the high-order scheme produces undershoots in velocity and internal energy while SFCR is free of undershoots and overshoots. The table of convergence is presented in Table 2 which also includes results by the S&S method [11]. SFCR is better than S&S, it is also better than the high-order method in velocity and internal energy and only slightly worse than the high-order method for density (SFCR convergence is better even for density). The SFCR order of convergence is about the same as that for the high-order method.

7. Conclusion

We have developed a new optimization-based synchronized flux corrected remapping of mass/density, momentum/velocity and specific internal energy to be used in the ALE methods. The main new results are derivation of a local linear objective function and new sufficient conditions for preservation of bounds on internal energy.

Acknowledgments

This work was performed under the auspices of the National Nuclear Security Administration of the US Department of Energy at Los Alamos National Laboratory under Contract DE-AC52-06NA25396. The authors gratefully acknowledge the partial support of the US DOE NNSA's Advanced Simulation and Computing (ASC) Program and the partial support of the US DOE Office of Science Advanced Scientific Computing Research (ASCR) Program in Applied Mathematics Research. The first and the third author have been supported in part by the Czech Ministry of Education grants MSM 6840770022 and LC528 and are grateful for support from the European Science Foundation OPTPDE Network on Optimization with PDE Constraints.

The authors thank P. Smolarkiewicz, D. Kuzmin, C. Schär, B. Kashiwa, T. Ringler, J. Shadid, L. Margolin and B. Rider for fruitful discussions and also anonymous reviewers for constructive comments.

References

[1] Hirt C, Amsden A, Cook J. An arbitrary Lagrangian–Eulerian computing method for all flow speeds. J Comput Phys 1974;14:227–53 [reprinted in 135(2);1997:203–16].
[2] Margolin L, Shashkov M. Second-order sign-preserving conservative interpolation (remapping) on general grids. J Comput Phys 2003;184:266–98.
[3] Shashkov M, Wendroff B. The repair paradigm and application to conservation laws. J Comput Phys 2004;198(1):265–77.
[4] Boris J, Book D. Flux-corrected transport. I: SHASTA, a fluid transport algorithm that works. J Comput Phys 1973;11:38–69.
[5] Zalesak S. Fully multidimensional flux-corrected transport algorithms for fluids. J Comput Phys 1979;31:335–62.
[6] Kuzmin D, Löhner R, Turek S, editors. Flux-corrected transport. Principles, algorithms and applications. Springer-Verlag; 2005.
[7] Zalesak S. The design of flux-corrected transport (FCT) algorithms for structured grids. In: Kuzmin D, Löhner R, Turek S, editors. Flux-corrected transport: Principles, algorithms, and applications. Springer-Verlag; 2005. p. 29–78.
[8] Kuzmin D, M öller M. Algebraic flux correction. II. Compressible Euler equations. In: Kuzmin D, Löhner R, Turek S, editors. Flux-corrected transport: principles, algorithms, and applications. Springer-Verlag; 2005. p. 207–50.
[9] Löhner R, Morgan K, Peraire J, Vahdati M. Finite element flux-corrected transport (FEM-FCT) for the euler and Navier–Stokes equations. Int J Numer Methods Fluids 1987;7:1093–109.
[10] Löhner R, Baum J. 30 Years of FCT: status and directions. In: Kuzmin D, Löhner R, Turek S, editors. Flux-corrected transport: principles, algorithms, and applications. Springer-Verlag; 2005. p. 131–54.
[11] Schär C, Smolarkiewicz P. A synchronous and iterative flux-correction formalism for coupled transport equations. J Comput Phys 1996;128:101–20.
[12] Váchal P, Liska R. Sequential flux-corrected remapping for ALE methods. In: de Castro AB, Gömez D, Quintela P, Salgado P, editors. Numerical mathematics and advanced applications. ENUMATH 2005. Berlin, Heidelberg, New York: Springer; 2006. p. 671–9.
[13] Liska R, Shashkov M, Váchal P, Wendroff B. Optimization-based synchronized flux-corrected conservative interpolation (remapping) of mass and momentum for arbitrary Lagrangian–Eulerian methods. J Comput Phys 2010;229(5):1467–97.